Comfurius, P., & Zwaal, R. F. A. (1977) *Biochim. Biophys. Acta 488,* 36–42.
Dawson, R. M. C. (1967) *Biochem. J. 102,* 205–210.
Demel, R. A., Jansen, J. W. C. M., Van Dijck, P. W. M., & Van Deenen, L. L. M. (1977) *Biochim. Biophys. Acta 465,* 1–10.
Hinz, H-J., & Sturtevant, J. M. (1972) *J. Biol. Chem. 247,* 3697–3700.
Jackson, C. M., Owen, W. G., Gitel, S. N., & Esmon, C. T. (1974) *Thromb. Diath. Haemorrh., Suppl. 57,* 273–293.
Jacobson, K., & Papahadjopoulos, D. (1975) *Biochemistry 14,* 152–161.
King, E. J. (1932) *Biochem. J. 26,* 292–299.
Lee, A. G. (1977) *Biochim. Biophys. Acta 472,* 285–344.
Luna, E. J., & McConnell, H. M. (1977) *Biochim. Biophys. Acta 470,* 303–316.
Papahadjopoulos, D., Jacobson, K., Nir, S., & Isac, T. (1973) *Biochim. Biophys. Acta 311,* 330–348.
Papahadjopoulos, D., Vail, W. J., Pangborn, W. A., & Poste, G. (1976) *Biochim. Biophys. Acta 448,* 265–283.
Phillips, M. C., Ladbrooke, B. D., & Chapman, D. (1970) *Biochim. Biophys. Acta 196,* 35–44.
Tocanne, J. F., Ververgaert, P. H. J. Th., Verkleij, A. J., & Van Deenen, L. L. M. (1974) *Chem. Phys. Lipids 12,* 201–219.
Van Dijck, P. W. M., Ververgaert, P. H. J. Th., Verkleij, A. J., Van Deenen, L. L. M., & de Gier, J. (1975) *Biochim. Biophys. Acta 406,* 465–478.
Verkleij, A. J., de Kruyff, B., Ververgaert, P. H. J. Th., Tocanne, J. F., & Van Deenen, L. L. L. (1974) *Biochim. Biophys. Acta 339,* 432–437.
Ververgaert, P. H. J. Th., de Kruyff, B., Verkleij, A. J., Tocanne, J. F., & Van Deenen, L. L. L. (1975) *Chem. Phys. Lipids 14,* 97–101.

Ligand-Induced Conformation Changes in *Torpedo californica* Membrane-Bound Acetylcholine Receptor†

U. Quast,‡ M. Schimerlik,§ T. Lee, V. Witzemann,‡ S. Blanchard,¶ and M. A. Raftery*

ABSTRACT: A time-dependent increase in ligand affinity has been studied in cholinergic ligand binding to *Torpedo californica* acetylcholine receptor by inhibition of the kinetics of [^{125}I]-α-bungarotoxin–receptor complex formation. The conversion of the acetylcholine receptor from low to high affinity form was induced by both agonists and antagonists of acetylcholine and was reversible upon removal of the ligand. The slow ligand induced affinity change in vitro resembled electrophysiological desensitization observed at the neuromuscular junction and described by a two-state model (Katz, B., & Thesleff, S. (1957) *J. Physiol. 138,* 63). A quantitative treatment of the rate and equilibrium constants determined for binding of the agonist carbamoylcholine to membrane bound acetylcholine receptor indicated that the two-state model is not compatible with the in vitro results.

The binding of AcCh[1] to the nicotinic AcChR results in an increase in the cation permeability of the postsynaptic membrane, thereby initiating postsynaptic depolarization at the neuromuscular junction. The preparation of membrane fragments enriched in AcChR from *Torpedo californica* (Duguid & Raftery, 1973) allows in vitro study of the interaction of this molecule in its membrane environment with ligands that depolarize (agonists) or that prevent depolarization (antagonists) in vivo. Inhibition of the time course of AcChR-[^{125}I]-α-Butx complex formation by ligands is a convenient method for studying these in vitro interactions since receptor-α-Butx complex formation is irreversible and a direct and simple assay procedure has been developed (Schmidt & Raftery, 1973).

It has been previously shown (Katz & Thesleff, 1957) that prolonged application of the agonists AcCh, Carb, or succinylcholine to frog sartorius muscle end plates resulted in decreased effectiveness of these agonists, although they were applied in doses large enough to usually cause depolarization. They termed this phenomenon "desensitization" and explained it by showing that the AcChR changed from an "effective" (low ligand affinity) to a "refractory" (high ligand affinity) state in the presence of ligand. Rang & Ritter (1969, 1970a,b) found that preincubation with agonists caused an increase in AcChR affinity for certain antagonists which was independent of the agonists that induced this "metaphilic effect". Using AcChR-rich membranes from *Torpedo marmorata,* Weber et al. (1975) have reported that preincubation with the agonists AcCh, Carb, and PTA induced a high affinity form of AcChR, while the antagonists d-TC and flaxedil did not, with Hexa and Deca causing this change in affinity toward Carb but not toward themselves. They concluded that the transition to the high affinity form of AcChR is induced primarily by agonists.

† Contribution No. 5351 from the Church Laboratory of Chemical Biology, Division of Chemistry and Chemical Engineering, California Institute of Technology, Pasadena, California 91125. *Received May 24, 1977; revised manuscript received March 1, 1978.* Supported by U.S. Public Health Service Grants NS10294 and GM16424.
‡ Recipient of a Deutsche Forschungsgemeinschaft Postdoctoral Fellowship.
§ Recipient of a National Institutes of Health Postdoctoral Fellowship NS 05145-02.
¶ Supported by a National Institutes of Health Training Grant GM 01262.

[1] Abbreviations used: AcCh, acetylcholine; AcChR, acetylcholine receptor; AcChE, acetylcholinesterase; α-Butx, α-bungarotoxin; Carb, carbamoylcholine; DAP, bis(3-aminopyridinium)-1,10-decane diiodide; DFP, diisopropyl fluorophosphate; Deca, decamethonium; Hexa, hexamethonium; d-TC, d-tubocurarine; PTA, phenyltrimethylammonium; *Torpedo* Ringers: 5 mM Tris-HCl buffer (pH 7.4) containing 250 mM NaCl, 5 mM KCl, 4 mM $CaCl_2$, and 2 mM $MgCl_2$; cpm, counts per minutes; [ ]$_0$ denotes total concentration.

0006-2960/78/0417-2405$01.00/0

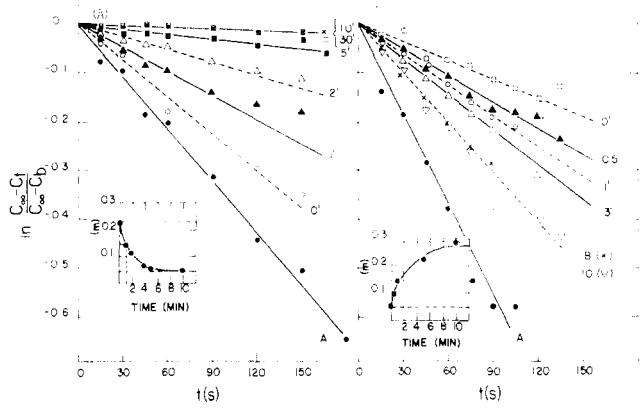

FIGURE 1: (Left) Time course of AcChR α-Butx complex formation in the presence of Carb. Data are presented in a normalized semilogarithmic plot $\ln[(C_\infty - C_t)/(C_\infty - C_b)]$ vs. time, where C_∞ and C_t are the experimental cpm at equilibrium and at time t (containing a constant background C_b, see Materials and Methods). AcChR (10^{-7} M in α-Butx binding sites) was incubated in the presence of Carb (10^{-6} M) in Ringers at 25 °C. At times indicated α-Butx (5×10^{-7} M) was added and the initial rates of toxin binding were determined. (A) Toxin binding rate in the absence of Carb. (Insert) Half-time of the conversion to high affinity form. Initial slopes of the semilog plots (m, in min^{-1}) were plotted vs. incubation time of AcChR with Carb. (Right) Recovery to low affinity AcChR after removal of Carb. AcChR (3×10^{-6} M α-Butx binding sites) in Ringers was incubated for 20 min at 25 °C with Carb (1.8×10^{-6} M) followed by a 40-fold dilution into Ringers without Carb, for recovery. After times indicated (0-10 min) α-Butx (5×10^{-7} M) and Carb (10^{-6} M) were added and the initial rate of toxin binding was measured. (Controls): (A) Dilution (×40) of AcChR, without preincubation with Carb, into Ringers without Carb; (B) AcChR diluted into Ringers containing toxin and Carb (10^{-6} M). (Insert) Half-time of recovery. Initial toxin binding rates (m) are plotted vs. time after dilution.

This transition has also been described by Lee et al. (1977) and treated quantitatively by Colquhoun & Rang (1976) and Weiland et al. (1976). Bonner et al. (1976) and Barrantes (1976) have detected slow changes in intrinsic fluorescence of the membrane bound receptor that occurred after agonist binding by stopped-flow measurements, while Grünhagen & Changeux (1976), Changeux et al. (1976), and Schimerlik & Raftery (1976) have detected conformational changes upon ligand binding using extrinsic fluorescent probes. Many of the above studies (e.g., Colquhoun & Rang, 1976; Weiland et al., 1976) were interpreted in terms of a two-state model, originally proposed by Katz & Thesleff (1957) for the neuromuscular junction, or a modified model which included the open channel receptor form (Grünhagen & Changeux, 1976; Lee et al., 1977). The time-dependent effects of agonists and antagonists on the rate of AcChR-[^{125}I]-α-Butx complex formation presented here indicate that this conversion from low to high affinity form(s) is not agonist specific. In addition, a quantitative treatment of the kinetic constants determined for the ligand Carb indicated that a two-state model was not adequate to explain these data.

Materials and Methods

Torpedo californica electric organs were excised after the animal was sacrificed and either used immediately or stored at −90 °C. AcChR-rich membrane fragments were prepared using procedures developed in this laboratory (Duguid & Raftery, 1973; Reed et al., 1975).

The concentration of α-Butx binding sites was determined by the DEAE-cellulose filter-disc assay procedure (Schmidt & Raftery, 1973) using [^{125}I] α-Butx prepared from purified α-Butx (Clark et al., 1972) obtained from *Bungarus multicinctus* venom (Sigma Chemical Co). All assays were conducted in prewashed plastic tubes which minimize adsorption of α-Butx to the tube walls (manuscript in preparation). Time courses for [^{125}I]-α-Butx binding were determined by pipetting 0.1 mL of the reaction mixture onto a DEAE filter disc (Whatman DE 81) and allowing to soak in, thus rapidly stopping the reaction (details to be published). The discs were washed three times for 10 min each in 10 mM sodium phosphate, pH 7.4, 0.1% Triton X-100, 50 mM NaCl and counted in a Packard scintillation counter optimized for ^{125}I. The counts at time t, C_t, are proportional to the amount of receptor–toxin complex formed when a constant background due to nonspecific binding of toxin (less than 0.5% of the total toxin) is subtracted. Since the difference $C_\infty - C_t$ is considered, the constant background cancels.

All membrane fragment preparations were routinely assayed to determine whether they were capable of undergoing the isomerization from low to high affinity form(s) for Carb. This was done by comparing the initial rate of [^{125}I]-α-Butx AcChR complex formation under conditions where [^{125}I]-α-Butx was in excess (see Figure 1) in the presence or absence of 1 μM Carb, with or without preincubation for 10 min. Membrane fragments were considered totally in the low affinity form when the initial rate of toxin binding in the absence of Carb equaled the rate determined in the presence of 1 μM Carb without preincubation. Preparations in which the initial rate of complex formation without incubation approached that found after incubation with 1 μM Carb were considered to be largely in the high affinity form and were discarded.

DAP was synthesized by the slightly modified (Witzemann & Raftery, 1977) procedure of Mooser et al. (1972); Carb and d-TC were purchased from Sigma Chemical Co., AcCh and DFP from Aldrich Chemical Co. and Deca and Hexa from K & K Labs, Inc., and Mann Research Lab, Inc., respectively. All experiments were done in *Torpedo* Ringers buffer unless otherwise stated, with the exact conditions listed in the figure captions.

The pharmacological action of DAP was examined by iontophoresis and bath application at the frog neuromuscular junction as well as by voltage jump relaxation studies on the *Electrophorus* electroplaque. In both systems, DAP is not an agonist and inhibits the response to agonists (H. A. Lester & D. Armstrong, unpublished results).

Data were analyzed using the method of weighted linear least squares. When nonlinear functions were fitted (e.g., eq 4 and 7), the weighting factors were recalculated to correct for the necessary linearizing transformation according to Bevington (1969). Propagation of errors in the determination of the calculated parameters was computed using standard methods (Bevington, 1969).

Results

Initial Observations. The time-dependent effects on the rate of [^{125}I]-α-Butx binding to AcChR enriched membrane fragments incubated with 1 μM Carb are shown in Figure 1A. There was a decrease in the initial rate of receptor–toxin complex formation as a function of incubation time. An apparent half-time of 80 ± 8 s for this process, under these conditions, was calculated from a semilog plot of the initial [^{125}I]-α-Butx binding rate vs. incubation time. Since Carb is an inhibitor of α-Butx binding (see below) and the bimolecular rate constant for Carb binding to the AcChR approaches the diffusion-controlled limit (Sheridan & Lester, 1975; Bonner et al., 1976), the time dependent change can be attributed to a slow conformational change of the AcChR–Carb complex

to a high affinity form for that ligand:

$$R + L \underset{}{\overset{K}{\rightleftharpoons}} RL \underset{k_{-1}}{\overset{k_1}{\rightleftharpoons}} R'L \qquad (1)$$

where R and R′ represent the low and high affinity forms of AcChR, L is the ligand, and $K = [R][L]/[RL]$.

That this conformational change was reversible upon dilution of the ligand is shown in Figure 1B. After incubation of receptor with Carb for 20 min, the AcChR was completely in the high affinity form (R′L) as determined by the assay procedure. The R′L complex was then diluted 40-fold (final $[Carb]_0 = 45$ nM) and the initial rate of α-Butx binding was determined by addition of 1 μM Carb plus α-Butx at various time intervals after dilution. Ten minutes after dilution the initial rate of toxin binding had returned to that found when low affinity AcChR was added to 1 μM Carb + α-Butx, indicating that the isomerization to the low affinity form was complete. From these data, the apparent half-time for recovery was determined to be approximately 120 s.

Additional experiments (see below, especially Figure 3) show that upon dilution the ligand dissociates rapidly from the high affinity form. Under these conditions the AcChR returns to the low affinity form essentially by the pathway shown in eq 2.

$$R'L \overset{\text{dilution}}{\rightleftharpoons} L + R' \underset{k_0}{\overset{k_{-0}}{\rightleftharpoons}} R + L \qquad (2)$$

Quantitative Examination of the Two-State Model. The initial results described above seemed compatible with the two state model of the AcChR (Katz & Thesleff, 1957) modified to include α-Butx binding to free AcChR forms (see also Lester, 1972; Weiland et al., 1976).

$$\begin{array}{ccc} & RT & \\ & T\uparrow k & \\ L + R & \overset{K}{\rightleftharpoons} & RL \\ k_0 \uparrow\downarrow k_{-0} & & k_{-1} \uparrow\downarrow k_1 \\ L + R' & \overset{K'}{\rightleftharpoons} & R'L \\ & T\downarrow k & \\ & R'T & \end{array} \qquad (3)$$

where $K_0 = k_0/k_{-0} = R'/R$, $K' = [R'][L]/[R'L]$, T = [^{125}I]-α-Butx, and RT and R′T = AcChR-[^{125}I]-α-Butx complex. k, the bimolecular rate constant for [^{125}I]-α-Butx binding, is equal for combination with both R and R′ (see below). The other terms have been defined in eq 1 and 2.

(A) Toxin Binding. Since we used [^{125}I]-α-Butx–AcChR complex formation as a probe for ligand induced conformational changes, it was important to examine the mechanism of toxin binding to the receptor and the relationship between toxin and Carb binding. In eq 3 we assume that (i) toxin binding to the membrane-bound AcChR is strictly bimolecular and irreversible, (ii) toxin and Carb are mutually exclusive, and (iii) the rate constants of toxin binding to the low and high affinity forms of the receptor are the same.

With respect to i, trace A in Figure 2A shows that with toxin concentrations in excess over receptor the kinetics of complex formation follows a single exponential over at least 90% of the reaction. The apparent rate constant varies linearly with toxin concentration in the accessible range from 0.25 to 1.5 μM (see Figure 2B, trace A). Isotopic dilution experiments show that the receptor–toxin complex does not dissociate over a period of 3 days (V. Witzemann, unpublished). At the toxin concentration normally used in our assays (0.5 μM), the reaction

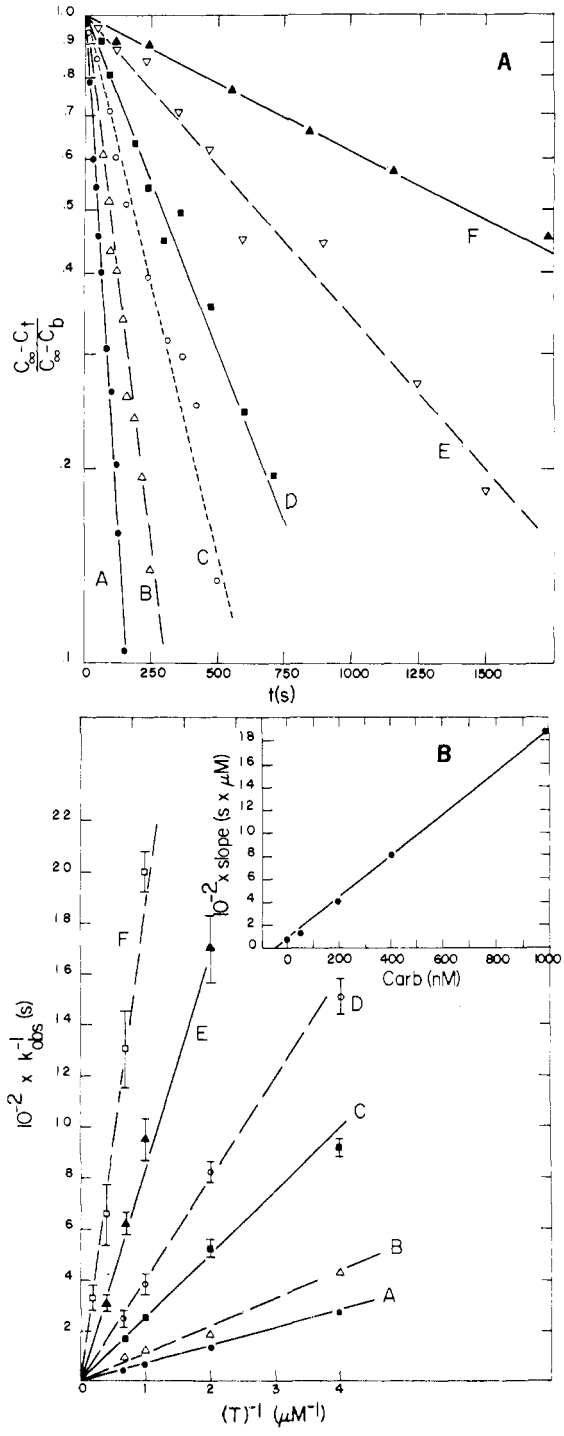

FIGURE 2: (A) Kinetics of toxin binding at different concentrations of Carb. Data are presented as normalized semilogarithmic plots of complex formation vs. time. AcChR (5×10^{-8} M in toxin sites), originally in the high affinity form, was preincubated with the amount of Carb indicated below for at least 30 min; then toxin was added (final concentration 1 μM). (●, A) Carb = 0, (△, B) 50 nM, (○, C) 100 nM, (■, D) 200 nM, (▽, E) 400 nM, (▲, F) 1 αM. Straight lines were calculated according to a linear least-squares fit and yielded the apparent rate constant of toxin binding k_{obsd}. (B) Double-reciprocal plot of k_{obsd} as function of toxin concentration at various Carb concentrations. The concentrations were: AcChR = 3×10^{-8} M in toxin sites at $T_0 = 2.5 \times 10^{-7}$ M and 5×10^{-8} M at all other toxin concentrations (T_0 = 0.5, 1, 1.5, 2, and 4 μM). k_{obsd} was obtained as described in Figure A. (●, A) No Carb, (△, B) Carb = 50 nM, (■, C) Carb = 100 nM, (○, D) 200 nM, (▲, E) 400 nM, (□, F) 1 μM. Straight lines were obtained by a weighted linear least-squares fit with the constraint of an ordinate intercept of 0. (Insert) Plot of the slopes determined above vs. free Carb concentration. From a weighted linear least-squares fit according to eq 4, one obtains after correction for the fraction of Carb bound $K_{app} = 50 \pm 10$ nM and the bimolecular rate of toxin binding $k = 1.5 \pm 0.3 \times 10^4$ M^{-1} s^{-1}.

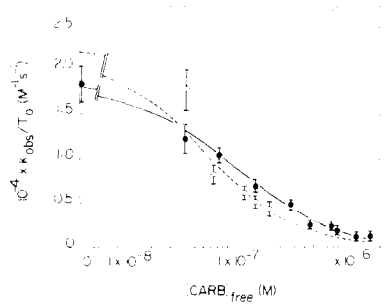

FIGURE 3: Inhibition of initial rate of toxin binding as a function of free Carb concentration after preincubation. The apparent bimolecular rate constant of toxin binding k_{obsd}/T_0 is plotted vs. free Carb concentration given on a logarithmic scale. (●) Data obtained with AcChR initially in the low affinity state. AcChR (7.3×10^{-8} M toxin sites) was preincubated with different Carb concentrations for at least 20 min to reach equilibrium. [^{125}I]-α-Butx was added (final toxin concentration = 5×10^{-7} M) at time zero and the kinetics of toxin binding was followed by disc assay. The total amount of AcChR–toxin complex formed, determined 15–20 h after toxin addition, was independent of Carb concentration. The initial rate of toxin binding k_{obsd} was determined from semilog plots by a linear least-squares fit. The solid line (——) is a fit of the experimental data according to eq 4 with $K_{app} = 0.12 \pm 0.02$ μM and $k = 1.8 \pm 0.2 \times 10^4$ M^{-1} s^{-1}, obtained by weighted linear least-squares fit to the linearized form of eq 4. The correction for the ligand bound never exceeded 20% and was achieved by an iterative procedure. (○) Data measured when starting from the high affinity state. AcChR (0.52 μM toxin sites) incubated in 1 μM Carb–Ringers for 45 min at 4 °C (AcChR was completely in the high affinity state by our assay conditions). It was diluted 40-fold into Ringers containing 0.26 μM [^{125}I]-α-Butx and a given Carb concentration (ranging from 0 to 0.2 μM) and the initial rate of toxin binding was determined (36 s as compared with a half-time of recovery of 120 s). The fit (- - -) of the experimental data (○) to eq 4 yielded $K_{app} = 57 \pm 8$ nM for the dissociation constant of the ligand to the high affinity receptor. From the ordinate intercept the rate of toxin binding to the high affinity receptor R′ equaled $2.2 \pm 0.3 \times 10^4$ M^{-1} s^{-1}.

of toxin with the membrane bound receptor is therefore described by a bimolecular irreversible binding mechanism to one homogeneous class of sites (see Discussion).

With respect to ii, after preincubation of receptor with Carb at various concentrations (see Figure 2A) toxin binding is inhibited by Carb and the kinetics still follow a single exponential. At high Carb concentrations the kinetics are slow and completion of the reaction is difficult to follow. Within the limited time range of interest (less than 20 min, see Figure 4A), the apparent rate of toxin binding in the presence of Carb (k_{obsd}) can be unambiguously defined (Figure 2A). Figure 2B shows the toxin dependence of k_{obsd} at different Carb concentrations in the form of a double-reciprocal plot. The data are fit by straight lines passing through the origin indicating a relationship of the form:

$$k_{obsd} = \frac{kT_0}{1 + L/K_{app}} \tag{4}$$

where T_0 is the toxin concentration (in large excess over toxin binding sites), L the free Carb concentration, and K_{app} the apparent equilibrium dissociation constant for Carb. This equation should be understood as an empirical formula and does not imply direct steric competition between Carb and toxin (see Discussion). A replot of the slopes in Figure 2B vs. free Carb concentration (Figure 2B, insert) gives $K_{app} = 50 \pm 10$ nM in agreement with the data shown in Figure 3 and the equilibrium constant for [^{3}H]Carb binding to membrane fragments as determined by centrifugation assay (Raftery et al., 1975). The bimolecular rate constant for toxin binding to this preparation of membrane fragments was $1.5 \pm 0.3 \times 10^4$ M^{-1} s^{-1}.

With respect to iii, the rate constants for toxin binding to the low and high affinity forms can be taken from the ordinate intercepts of the fitted lines in Figure 3. It is seen that within the experimental error both R and R′ bind toxin with approximately the same rate constant $k = 2 \pm 0.2 \times 10^4$ M^{-1} s^{-1} (see legend of Figure 3). A similar observation was reported by Weber et al. (1975) and Weiland et al. (1976).

(B) Equilibrium Conditions. Assuming eq 3 represented the correct kinetic model, K and K' were determined as follows: AcChR-rich membrane fragments in the low affinity form were incubated with various Carb concentrations until equilibrium was reached (20–30 min) and the reaction was started by addition of an excess of [^{125}I]-α-Butx. The initial rate of [^{125}I]-α-Butx-AcChR formation was determined from a semilog plot of $C_\infty - C_t$ vs. time. From eq 3, the apparent equilibrium constant for Carb binding to R is approximately $K_{app} \simeq K \times k_{-1}/k_1$ since $k_{-1}/k_1 \ll 1$ (see below). Microscopic reversibility in eq 3 requires that $K \times k_{-1}/k_1 = K'/K_0$ and a value of K'/K_0 equal to 0.12 ± 0.02 μM was determined from a fit of the data shown in Figure 3 (●, ——) to eq 4.

For the determination of K' the AcChR was incubated with an excess of Carb (1 μM) so that it was converted to the high affinity form as verified experimentally. The mixture was then diluted into solutions of varying Carb concentrations plus [^{125}I]-α-Butx, to start the reaction. Since the initial rate of toxin binding is fast compared with reisomerization to the low affinity form but slow compared with ligand dissociation, it follows the pathway:

$$\underset{L + T}{R'L} \xrightarrow{\text{dilution into}} \underset{T}{L + R'} \xrightarrow{k} R'T \tag{5}$$

The experimental data are shown in Figure 3 (○). The fit of these data to eq 4 where $K_{app} = K'$ gave $K' = 57 \pm 8$ nM. From the ordinate intercepts of the fitted curves the bimolecular rate constants for [^{125}I]-α-Butx binding to R and R′ were equal to $1.8 \pm 0.2 \times 10^4$ M^{-1} s^{-1} and $2.2 \pm 0.3 \times 10^4$ M^{-1} s^{-1}, respectively (see Figure 3). Using the values of K' and K'/K_0, K_0 was calculated to equal 0.48 ± 0.10 for this experiment. In equilibrium binding studies with [^{3}H]Carb, this result has been confirmed and values closer to one have occasionally been observed (M. Schimerlik, in preparation). Since the membrane fragments were initially in the low affinity form ($K_0 < 0.1$ as determined in the assay procedure described in Materials and Methods), this result is in clear contradiction to the two-state model (eq 3).

(C) Kinetic Studies. In a separate set of experiments the apparent rate constant for the isomerization from low to high affinity form, k_i, was determined as a function of Carb concentration. At Carb concentrations less than 5 μM, the initial rate of [^{125}I]-α-Butx binding was sufficiently faster than the apparent rate of isomerization to the high affinity form and conditions where toxin was in large excess over receptor were applicable (see Appendix). However, at higher levels of Carb the conversion of the receptor to high affinity form was faster than the initial rate of toxin binding and experimental conditions where AcChR was in excess over [^{125}I]-α-Butx had to be used (see Appendix and Figure 4A). Then it was possible to study the Carb concentration dependence up to 20 μM (Figure 4B). As shown in Figure 4A the time course of toxin binding under these conditions followed that predicted in eq A16 and allowed a convenient determination of k_i.

The Carb dependence of the rate of isomerization, k_i, is shown in Figure 4B. At higher Carb concentrations k_i starts to level off as predicted by eq A13 which states that

$$k_i = \frac{k_0 + k_1 L/K}{1 + L/K} + \frac{k_{-0} + k_{-1} L/K'}{1 + L/K'} \tag{6}$$

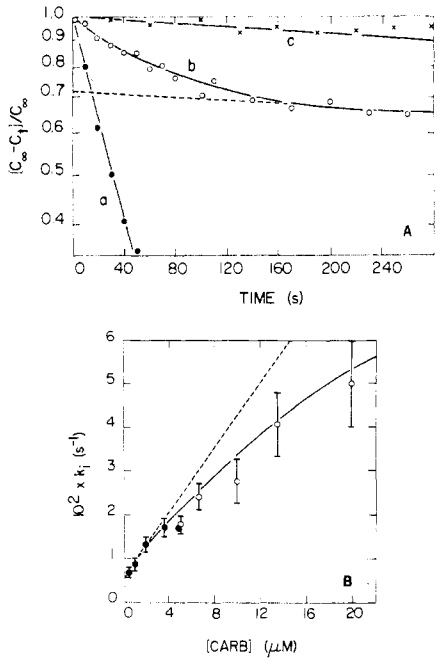

FIGURE 4: (A) Kinetics of transition to high affinity form with AcChR in excess at 5 μM Carb. AcChR = 0.88 μM; [^{125}I]-α-Bgt = 9.4×10^{-8} M. A semilog plot of the data $[C_\infty - C_t]/C_\infty$ vs. time is shown. Time course a (●): addition of toxin to AcChR at time zero. From a linear least-squares fit, a toxin on rate $k = 2.2 \pm 0.3 \times 10^4$ M^{-1} s^{-1} is calculated. Time course b (○): simultaneous addition of toxin and 5 μM Carb to AcChR. The fast initial decrease reflects the transition to high affinity form; the linear slope at the end of the curve shows the (slow) binding of toxin to the receptor now completely in high affinity form for Carb. According to eq A16, a semilog plot of the deviation of the actual time course from its asymptotic linear slope directly yields the rate of transition to high affinity form. The weighted linear least-squares fit gives $k_i = 1.8 \pm 0.2 \times 10^{-2}$ s^{-1}. Time course c (X) shows toxin binding to receptor which was preincubated for 20 min with 5 μM Carb. The apparent rate of toxin binding is the same as the limiting slope of time course b. From the linear least-squares fit one obtains an apparent toxin on rate $k_{app} = 3.8 \pm 1.0 \times 10^{-4}$ s^{-1} as compared with the calculated value $k_{app} = 4.2 \times 10^{-4}$ s^{-1} (using eq 4 and $K_{app} = 0.12$ μM). (B) Apparent rate of conversion to high affinity form, k_i, as a function of Carb concentration. (●) High toxin kinetics, conditions similar to those in Figure 1A; (○) high receptor kinetics as shown in A. The error bars show the standard error obtained from the linear least-squares fits of the raw data to a single exponential from which the values of k_i at different Carb concentrations were determined. Data were fitted by weighted least squares to a linearized form of eq 7 $(k_i - k_{-1})^{-1} = k_1^{-1}(1 + K/L)$ from which $k_{-1} = 6 \pm 1 \times 10^{-3}$ s^{-1}, $k_1 = 0.14 \pm 0.04$ s^{-1}, and $K = 40 \pm 14$ μM were obtained. The solid curve is a plot according to eq 7 using these parameters. The broken line represents the initial slope of eq 7 (for $L \ll K$) with a slope $k_1/K = 3.6 \pm 0.7 \times 10^3$ M^{-1} s^{-1}, calculated from the above parameters.

In general, k_i will be a nonmonotonic function of ligand concentration (Janin, 1973). In this case, however, the pertinent parameters can be obtained by the following argument: from the half time of recovery $T_{1/2} \simeq 120$ s (Figure 1B) we can roughly estimate $k_0 + k_{-0} = k_{-0}(1 + K_0) \simeq \ln 2/120$ $(s^{-1}) \leq 10^{-2}$ s^{-1} so that $k_0 < k_{-0} < 1 \times 10^{-2}$ s^{-1}. At higher ligand concentrations $L \geq 1$ μM we have $L/K' \geq 20$ and the terms in eq 6 containing k_0 and k_{-0} can be neglected to a good approximation since $k_i \geq 10^{-2}$ s^{-1}. Thus eq 6 can be written as:

$$k_i = \frac{k_1 L/K}{1 + L/K} + k_{-1} \qquad (7)$$

This function can be unambiguously extrapolated toward $L \rightarrow 0$ and from the experimental data in Figure 4B one determines that $k_{-1} = 6 \pm 1 \times 10^{-3}$ s^{-1}. Since the concentration range where k_i levels off completely could not be reached experimentally, the parameters K and k_1 were obtained from a linear least-squares fit to the linearized form of eq 7 (see Figure 4B for details). The value of K, the dissociation constant for Carb binding to the low affinity form, was found to be 40 ± 14 μM, in excellent agreement with the data of Bonner et al. (1976) and Popot et al. (1976). k_1, the unimolecular rate constant for the isomerization of AcChR-Carb to the high affinity form, equaled 0.14 ± 0.04 s^{-1} which is in fair agreement with the data of Bonner et al. (1976; $k_1 = 0.37$ s^{-1}). Inserting these parameters determined from the fit to eq 7 and using the experimental value $K_0 = 1/2$, curves can be calculated according to eq 6 by varying k_{-0}. Values of $k_{-0} = 4 \pm 3 \times 10^{-3}$ s^{-1} were compatible with the experimental data. From the parameters in eq 7 the overall equilibrium constant for Carb binding to receptor originally in the low affinity form is calculated to be $K_{ov} \simeq K k_{-1}/k_1 = 1.7 \pm 0.8$ μM. This value is more than tenfold higher than the directly determined value of 0.12 μM, demonstrating clearly that the two-state model is incompatible with the experimental data.

TABLE I: Reduction of the Initial Rate of [^{125}I]-α-Butx Binding by Cholinergic Ligands in the Case of No (A) or 10 Min (B) Preincubation.[a]

Ligand	Pharmacol. act.	Concn (M)	A (%)	B (%)	A/B
Carb	Agonist	1×10^{-6}	70	3.7	19.0
AcCh	Agonist	1×10^{-7}	44	16	2.8
Choline	Agonist[b]	1×10^{-4}	68	14	4.9
DAP	Antagonist[c]	1×10^{-5}	63	28	2.3
Hexa	Antagonist	1×10^{-4}	56	56	1.0
d-TC	Antagonist	2.8×10^{-7}	42	42	1.0

[a] $[AcChR]_0$ ranged from 5×10^{-8} M to 9×10^{-8} M in toxin sites, $[T]_0 = 5 \times 10^{-7}$ M. In the case of AcCh, the membrane fragments (3.6 μM in toxin sites) were preincubated for 1 h at room temperature with 2 mM DFP, resulting in complete inhibition of AcChE activity. The initial rates of toxin binding were determined from semilog plots in the absence of ligand (V_0) and in the presence of ligand without (V_1) and with preincubation (V_1'). A and B were calculated as $A \equiv V_1/V_0$ and $B \equiv V_1'/V_0$ (in %). [b] Adams (1975). [c] See Materials and Methods section.

Ligand Specificity. In order to determine the ligand specificity for inducing the conformational change(s), related to interconversion of receptor forms of differing ligand affinity, the time-dependent effects of a variety of agonists and antagonists were examined. The agonists AcCh (10^{-7} M) and choline (10^{-4} M) as well as the antagonist DAP (see Materials and Methods, 10^{-5} M) inhibited the initial rate of [^{125}I]-α-Butx-AcChR complex formation to a greater degree after a 10-min preincubation than without preincubation (see Table I). In addition, it was found that 10-min incubation with 10^{-4} M choline followed by a tenfold dilution into 1 μM Carb plus [^{125}I]-α-Butx caused the same inhibition of the initial rate of toxin binding as that found upon diluting untreated receptor into 1 μM Carb followed by further incubation before addition of toxin. This indicated that choline induced the conformational change from a low to high affinity form toward Carb.

Preincubation with the antagonist DAP also converted the AcChR to the high affinity form for Carb as shown in Figure 5A. The rate of [^{125}I]-α-Butx binding to membrane fragments which were preincubated for 20 min with 10 μM DAP and then diluted 50-fold into 1 μM Carb plus toxin was strongly inhibited (time course 4). Only a slightly stronger inhibition of the toxin binding rate was observed when the DAP treated membrane fragments were diluted into 1 μM Carb and preincubated an additional 20 min before addition of toxin (time

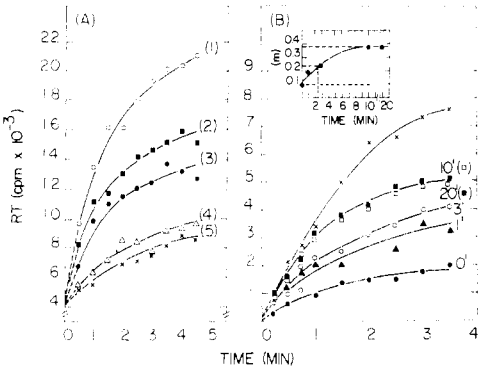

FIGURE 5: (A) Antagonist (DAP)-induced conversion of AcChR to high affinity toward agonist Carb. In all assays, the concentrations of AcChR and [^{125}I]-α-Butx were 6.4 ± 10^{-7} M and 5.1×10^{-6} M, respectively. (1) [^{125}I]-α-Butx binding in the absence of ligands. Membrane fragments were added at time zero to [^{125}I]-α-Butx in *Torpedo* Ringers. (2) Membrane fragments were added at time zero to 10^{-6} M Carb plus [^{125}I]-α-Butx. (3) Membrane fragments preincubated with 10^{-5} M DAP, diluted 50× (2×10^{-7} M final DAP) and incubated an additional 20 min before simultaneous addition of Carb (to 10^{-6} M) and [^{125}I]-α-Butx at time zero. (4) Membrane fragments preincubated with DAP as in 3, diluted (50×) into 10^{-6} M Carb plus [^{125}I]-α-Butx at time zero. (5) Membrane fragments preincubated as in 3, diluted (50×) into a solution containing 10^{-6} M Carb and incubated an additional 20 min before addition of [^{125}I]-α-Butx at time zero. (B) Recovery of AcChR converted to high affinity form by DAP. AcChR (4.1 μM) in Ringers was incubated for 20 min at 25 °C with DAP (2.2×10^{-5} M) followed by a 100-fold dilution into Ringers for recovery. After times indicated (0–20 min) the time course of toxin binding was measured upon addition of [^{125}I]-α-Butx and Carb at the same time. Final concentrations were: [AcChR] = 4×10^{-8} M, [^{125}I]-α-Butx = 5×10^{-7} M, [Carb] = 10^{-6} M. Time course (X) shows toxin binding in the absence of DAP and Carb. Insert showing half-time of recovery was obtained as in Figure 1.

TABLE II: Effects of Preincubation with Hexa.[a]

Ligand	v (%)	v_1 (%)	v_{11} (%)	$v_{11'}$ (%)	$\frac{v_{11}}{v_{11'}} - 1$
Carb (1 μM)	100	100	56	24	1.4
DAP (10 μM)	100	81	31	31	0.0
Deca (1 μM)	100	84	52	52	0.0

[a] v, initial velocity of RT formation in the absence of ligands normalized to 100%. v_1, initial rate of RT formation in the presence of the given ligand concentration without preincubation (normalized with respect to v, in %). v_{11}, initial rate of RT formation at the given ligand concentration after 15-min preincubation with 100 μM Hexa, diluted into ligand + [^{125}I]-α-Butx (final [Hexa] = 2.5 μM) at time zero (normalized). $v_{11'}$, initial rate of RT formation when the AcChR diluted as for v_{11}, was preincubated an additional 15 min with the ligand at the stated concentration and [^{125}I]-α-Butx added at time zero (normalized). $(v_{11}/v_{11'}) - 1$, a measure of the degree of inhibition caused by preincubation with 100 μM Hexa; a value of 0 indicates that preincubation with Hexa induced the AcChR conformational change to the same degree as preincubation with the ligand itself. All reactions were assayed in 1.0 mL of Ringers, 5.1×10^{-7} M [^{125}I]-α-Butx; AcChR, 8.7×10^{-8} M for DAP experiments, 8.1×10^{-8} M for Deca.

course 5). Thus, preincubation of AcChR with an antagonist (DAP) caused an increased affinity of the receptor for an agonist (Carb). Figure 5A also shows that this effect was reversible upon dilution of DAP. When DAP-treated membrane fragments were diluted into buffer alone followed by a 20-min incubation and subsequent addition of Carb plus toxin (time course 3), almost the same rate of toxin binding was observed as for membrane fragments which had never been exposed to DAP (time course 2). The time course of recovery from DAP-induced isomerization is shown in Figure 5B. The

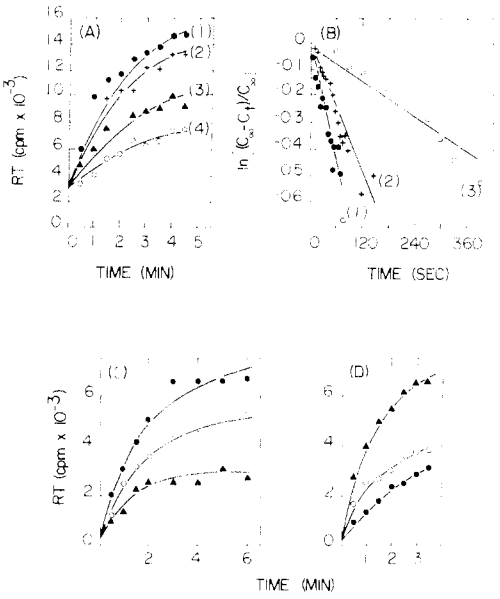

FIGURE 6: (A) Hexamethonium induced conversion of AcChR to high affinity form toward carbamoylcholine. In all cases [AcChR]$_0$ = 8×10^{-8} M toxin sites; [^{125}I]-α-Butx = 5.1×10^{-7} M; 1.0 mL total volume in *Torpedo* Ringers, pH 7.4. (1) Membrane fragments were added to [^{125}I]-α-Butx at time zero. (2) Receptor added to toxin plus 1 μM Carb. (3) Membrane fragments were preincubated 20 min in the presence of 10^{-4} M Hexa, and then diluted 40-fold into 10^{-6} M Carb plus [^{125}I]-α-Butx, ([Hexa]$_0$ = 2.5×10^{-6} M). (4) Membrane fragments preincubated as in 3 were diluted into 10^{-6} M Carb and incubated an additional 15 min before addition of [^{125}I]-α-Butx at time zero. (B) Determination of apparent K and K' for Hexa. All reaction mixtures were 3.2×10^{-8} M in α-Butx sites, 2.6×10^{-7} M in [^{125}I]-α-Butx. Semilog plots of toxin binding kinetics are shown for: (1) AcChR added to [^{125}I]-α-Butx at time zero; (2) AcChR added to [^{125}I]-α-Butx plus 100 μM Hexa at time zero; (3) AcChR preincubated with 1 μM Carb, diluted a 100-fold (final Carb concentration = 10^{-8} M) into 100 μM Hexa plus [^{125}I]-α-Butx at time zero. The amount of [^{125}I]-α-Butx AcChR complex at $t = \infty$ (5 h) was the same for all three time courses. The lines are drawn from a least-squares fit assuming an ordinate intercept = 0 and gave for k_{obsd} (1) $7.2 \pm 0.5 \times 10^{-3}$ s^{-1}, (2) $4 \pm 0.5 \times 10^{-3}$ s^{-1}, (3) $1.2 \pm 0.5 \times 10^{-3}$ s^{-1}. (C) d-TC induced conversion of AcChR to high affinity form toward Carb. Final concentrations were in all cases [d-TC] = 0.28 μM, [Carb] = 1 μM, [AcChR] = 0.06 μM. (●) Reaction started by adding AcChR to a mixture of Carb, d-TC, and [^{125}I]-α-Butx. (○) AcChR preincubated with 0.28 μM d-TC, followed by addition of Carb and [^{125}I]-α-Butx. (▲) AcChR preincubated with 0.28 μM d-TC and 1 μM Carb, followed by addition of [^{125}I]-α-Butx. (D) Toxin binding kinetics of low and high affinity AcChR in presence of d-TC. AcChR was first preincubated with 2.5 μM Carb and then diluted into the following media. (▲) Buffer, incubated for 20 min. [^{125}I]-α-Butx was then added. (●) d-TC and [^{125}I]-α-Butx. (○) Buffer, incubated for 20 min; d-TC and [^{125}I]-α-Butx was then added. Final concentrations: [d-TC] = 2.2 μM (zero in A); [Carb] = 0.06 μM; [^{125}I]-α-Butx = 0.5 μM; [AcChR] = 0.04 μM.

membrane fragments, preincubated 20 min with 22 μM DAP, were diluted a 100-fold to a final DAP concentration of 0.22 μM, and 1 μM Carb plus [^{125}I]-α-Butx were added at the time indicated. After 10 min the AcChR had reverted to the low affinity form for Carb with a half-time (Figure 5B, insert) of 140 ± 15 s. This agrees with the half-time for recovery from the high affinity state induced by Carb (Figure 1B), suggesting that the rate-determining step for AcChR isomerization from a high to a low affinity form was independent of whether the high affinity state was induced by an agonist (Carb) or an antagonist (DAP).

The antagonist Hexa, at concentrations less that 100 μM, did not strongly inhibit the time-course of [^{125}I]-α-Butx binding to membrane fragments, with or without preincubation (see Table I). Hexa could, however, induce tighter binding of other ligands to the receptor. This is shown in Figure 6A where

incubation of membrane fragments with 100 μM Hexa for 20 min followed by 50-fold dilution into 1 μM Carb plus toxin (final Hexa concentration of 2.5 μM, time course 3) resulted in stronger inhibition of the rate of toxin binding than dilution of untreated receptor into 1 μM Carb plus toxin (time course 2). The inhibition was even stronger when membrane fragments were incubated in 100 μM Hexa, diluted 40-fold into 1 μM Carb, and incubated an additional 15 min before the addition of toxin (time course 3). The effects of incubation of receptor with Hexa on the inhibition by other ligands of the toxin binding kinetics are summarized in Table II. Clearly, Hexa converted the AcChR to a high affinity form for the agonists Carb and Deca as well as for the antagonist DAP since the initial rate of toxin binding upon preincubation of receptor with 100 μM Hexa followed by dilution into ligand plus toxin (v_{II}) was significantly lower than that observed without preincubation with Hexa (v_I). For DAP and Deca preincubation of receptor with Hexa induced the same effect as did further incubation with these ligands while further incubation with Carb induced a greater effect (see Table II). The values presented in Table II varied slightly with the membrane preparation and should be interpreted in a qualitative rather than quantitative manner. However, the data do indicate that a high affinity form(s) of AcChR could be induced by both agonists and antagonists.

Since Hexa induced (at least partially) the conversion of the AcChR to a high affinity form for other ligands, but showed no time dependent effects toward itself, it was of interest to determine the apparent dissociation constants for Hexa for both the low (K) and high (K') affinity receptor forms using eq 4.

In the absence of Hexa and with toxin in excess over receptor the observed rate of toxin binding is $k_{obsd} = kT_0$ (Figure 6B, time course 1). Therefore K and K' may be calculated by taking the slope of lines 2 and 3 in Figure 6B which represent the apparent rate of toxin binding to the low and high affinity form of AcChR in the presence of 100 μM Hexa. From the numbers given in the legend of Figure 6B, K and K' were calculated according to eq 4 to be 125 ± 47 μM and 20 ± 10 μM, respectively. Assuming that the two-state model applies for Hexa, one calculates the degree of desensitization I induced by 100 μM Hexa to be 86% (using eq A6 with $K_0 = \frac{1}{2}$, $K' = 20$ μM, and $K = 100$ μM). In contrast, Hexa does not increase the affinity toward itself upon preincubation despite a ratio of $K/K' = 6$, indicating again that a two-state model cannot account for the complicated phenomena observed.

d-TC like Hexa did not induce tighter binding toward itself upon preincubation with AcChR (see Table I). However, as shown in Figure 6C, AcChR preincubated with 0.28 μM d-TC did exhibit a slower [^{125}I]-α-Butx binding time course than nonpreincubated AcChR when Carb and [^{125}I]-α-Butx were added simultaneously to start the reaction (final $[Carb]_0 = 1$ μM). Toxin binding was even slower when the AcChR was incubated further with Carb (Figure 6C, ▲).

In Figure 6D, AcChR preincubated with 2.5 μM Carb was diluted into buffer containing 2.2 μM d-TC. As can be seen, toxin binding in the presence of 2.2 μM d-TC was only slightly slower when AcChR was in the high affinity state (Figure 6D, ●) than after recovery to the low affinity form(s) (Figure 6D, ○).

Discussion

Data presented in Figure 1 clearly show that the AcChR undergoes a reversible conformational change to a high affinity form upon incubation with the agonist Carb. This effect is generally believed (Lester, 1972; Weber et al., 1975; Bonner et al., 1976; Weiland et al., 1976; Colquhoun & Rang, 1976; Lee et al., 1977) to be an in vitro correlate of in vivo desensitization, observed at the neuromuscular junction and described by the two-state model (eq 3; Katz & Thesleff, 1957). This model was qualitatively consistent with our experimental observations assuming that eq 1 described the isomerization from the low to high affinity form upon addition of Carb and that the recovery to the low affinity form upon dilution of the R′L complex followed eq 2. It was possible to test this model using the kinetics of [^{125}I]-α-Butx-AcChR complex formation once toxin binding kinetics and its relationship with Carb binding were characterized. The data in Figure 2 show that, in the micromolar range, toxin combines in a strictly bimolecular manner with one homogeneous population of sites in the membrane fragments to form an irreversible complex. These results differ from our observations with solubilized purified receptor for which toxin binding revealed the existence of two different classes of sites (Raftery et al., 1975, also manuscript in preparation).

Equilibrium experiments with [^{3}H]Carb binding to membrane fragments have shown that there are half as many high affinity sites for Carb ($K_D \simeq 70 \pm 20$ nM) as there are [^{125}I]-α-Butx sites (Raftery et al., 1975; Quast et al., 1978; Schimerlik et al., in preparation). The apparent competitive inhibition of toxin binding by Carb is therefore a rather surprising result. Weber & Changeux (1974) have also observed that binding of *Naja naja* toxin and Carb is mutually exclusive. This finding is further supported by the complete absence of high affinity binding of [^{3}H]Carb to receptor toxin complex (Schimerlik et al., in preparation).

Our results clearly show that Carb and toxin are mutually exclusive at equilibrium. It is, however, experimentally very difficult to determine whether the precomplex RL (eq 1 and 3) can bind toxin. As shown in the Appendix (eq A9a), inclusion of ternary transient complexes TRL and T_2RL, formed with an arbitrary rate constant from RL and T, does not affect the observed rate constants for conversion from a low to a high affinity state and therefore leaves calculated parameters unchanged.

Analysis of the data in Figures 3 and 4B showed that the overall equilibrium constant, $K_{ov} \simeq Kk_{-1}/k_1$, calculated from kinetic experiments equaled 1.7 ± 0.8 μM (Figure 4B, eq 7). This is more than tenfold higher than the value of 0.12 ± 0.02 μM directly determined by inhibition of toxin binding after incubation of low affinity AcChR with Carb (Figure 3). The kinetically determined overall equilibrium constant agrees very well with the value $K_{ov} = 1.78$ μM determined by Bonner et al. (1976) by stopped-flow experiments. In their communication on the transition of AcChR toward the high affinity form, Weber et al. (1975) estimated an increase in affinity of low affinity AcChR toward Carb upon preincubation up to about 20-fold ($k_{-1}/k_1 \geq 5 \times 10^{-2}$) which together with the dissociation constant of Carb with low affinity AcChR determined in that laboratory ($K \simeq 50$ μM, Popot et al. (1976)) yields $K_{ov} \simeq 2$ μM. It seems that the kinetic data from different laboratories obtained with different techniques all give a value of $K_{ov} \simeq 1.5$ μM, whereas experiments performed after preincubation of membrane fragments with Carb give values of K_{ov} between 50 and 120 nM, regardless of the original affinity state of the receptor, as measured by [^{3}H]Carb binding (Raftery et al., 1975; Quast et al., 1978) or toxin inhibition (Figure 3 this communication or Weiland et al. 1976). A plausible way of resolving this apparent inconsistency seems to be to expand the two-state model to a three-state model by assuming a third state R″L which follows formation of R′L.

Formation of R″L could account for the discrepancy of a factor of 20 between the kinetic and thermodynamic determination of the equilibrium constant. Moreover, if one assumes that formation of R″L is much faster than the preceeding formation of R′L it is easy to show that the additional step R′L → R″L has a negligible amplitude in a kinetic scheme where the signal is proportional to the concentration of free receptor and that it can therefore not be directly observed.

Inclusion of a third state in this form does not, however, resolve the problem caused by the preexistence of the low and high affinity forms of the receptor R and R′ in the absence of ligand as required in a cyclic model. The equilibrium studies (Figure 3) starting with AcChR in the low affinity form ($K_0 \leq 0.1$) or high affinity form permit calculation of $K_0 = R'/R = 0.48$. This value is inconsistent with the experimental observation that in the absence of ligand the AcChR can be found essentially in the low affinity form (Figure 1A). We conclude that the two-state model (eq 3) gives a qualitative picture of the events occurring; however, the internal inconsistencies found for Carb indicate that this model is too simple to quantitatively account for the experimental observations in vitro. Stopped-flow experiments using the fluorescent probe ethidium bromide show indeed that the kinetics of Carb binding to membrane fragments is very complex and involves more than two states (Quast et al., 1978).

The antagonist DAP (see Table I) and the in vitro antagonist (Popot et al., 1976) Deca (Table II) induce, at least partially, the isomerization of the receptor to a high affinity form toward themselves and DAP induced the high affinity form of the receptor for Carb as well (See Figure 5). This differs from the results of Weber et al. (1975) who reported that desensitization was agonist specific. Hexamethonium (Figure 6A,B) and d-TC (Figure 6C,D) cause this conformational change to a lesser degree. This might be due to a higher ratio k_{-1}/k_1 in eq 1 and this can also be seen in the qualitative sense from eq 3 and A3 since, according to the two-state model, the extent of desensitization for any ligand would be dependent on the ratio of K/K' which is approximately 6 for Hexa but 1000 for Carb—the highest ratio for any ligand examined.

The half-time for recovery after dilution was the same for the agonist Carb and the antagonist DAP. In addition, agonists and antagonists could induce the high affinity form of AcChR toward each other (e.g., Figures 5A and 6, Table II). This might suggest that the same high affinity AcChR state was formed regardless of ligand; however, it is not yet possible to exclude a mechanism where each ligand partitions the AcChR-ligand complex between several high affinity states. In the latter case the rate-limiting step in recovery for both DAP and Carb induced AcChR high affinity forms must have the same rate constant or the limiting step in reisomerization to the low affinity form must proceed through a common intermediate.

In conclusion, the time-dependent effects of agonists and antagonists on the rate of [^{125}I]-α-Bgt binding to the AcChR have been studied. Both agonists and antagonists cause the conversion of the AcChR to the high affinity form(s) but to different degrees with Carb being the most efficient (highest value of K/K') of the compounds studied. A quantitative kinetic analysis of the Carb effects indicates that, while the in vitro effects seem to correspond to the in vivo phenomenon of desensitization, the two-state model initially proposed by Katz & Thesleff (1957) for observations at the neuromuscular junction does not adequately explain the in vitro observations using *Torpedo californica* membrane fragments. Other models, involving more than one molecule of ligand bound per AcChR molecule are currently under consideration.

Note Added in Proof

While this manuscript was being revised, a paper from P. Taylor & co-workers appeared (G. Weiland et al., 1977), dealing with the kinetics of desensitization as followed by the time-dependent inhibition by Carb of toxin binding kinetics to the AcChR from *Torpedo californica*. Although the experimental approach of these authors is similar to ours, they found their results in agreement with the two-state model. This discrepancy may be due to the following two reasons. (1) Difference in ionic conditions: Weiland et al. conducted their study in Ca^{2+}-free buffer (0.1 M NaCl, 10 mM sodium phosphate, pH 7.4), whereas our experiments were done in the presence of 4 mM $CaCl_2$ (*Torpedo* physiological Ringers). Ca^{2+} is, however, a very special ligand which induced fivefold tighter binding of Carb to the membrane bound receptor (Schimerlik et al., in preparation; a twofold increase in affinity for AcChR has been observed by Weber & Changeux, 1974). Therefore, the parameter values obtained by Weiland et al. cannot be directly compared with ours. (2) Different treatment of data: after having determined K, K', and K_{ov}, Weiland et al. fit their time courses of toxin binding in the presence of Carb to the two-state model by computer simulation assuming (a) K_0, $K_1 < 0.1$ and (b) using the constraint of microscopic reversibility, thus deriving the elementary rate constants k_1' and k_{-1}' appearing in eq A13. We determined these rate constants from the concentration dependence of k_i (Figure 4B) and found a tenfold discrepancy between the directly determined (see Figure 3) and the calculated ($K_{ov} = K \times k_{-1}/k_1$) values for K_{ov}.

Acknowledgment

The authors are grateful to Dr. H. A. Lester and D. Armstrong at the California Institute of Technology for performing the electrophysiological experiments involving DAP.

Appendix

The two-state model has been extensively treated in the literature (see e.g., Janin, 1973). It accounts only for one ligand molecule binding per macromolecule. Since two molecules of Carb bind to one receptor (Raftery et al., 1975), the symbol R in the equations of this paper stands for one-half of the whole multisubunit receptor. In addition to the notation introduced in eq 3, the abbreviations:

$$Q = [1 + L/K]^{-1}; Q' = [1 + L/K']^{-1} \quad \text{(A1)}$$

will be used. We will assume for the allosteric constant $K_0 \equiv R'/R \ll 1$ and we will consider the case of a "strong effector" like Carb for which the ratio K/K' is large enough to overcome the unfavorable ratio R'/R:

$$K_0 \ll 1 \ll K_0 K/K' \quad \text{(A2)}$$

Equilibrium Properties. In the absence of toxin the fraction of ligand bound is given by:

$$Y = [RL + R'L]/R_0 = LR'[K'^{-1} + (K_0 K)^{-1}]/R_0 \quad \text{(A3)}$$

Conservation of receptor sites can be written as $R_0 = R' \times [Q'^{-1} + (K_0 Q)^{-1}]$. Neglecting small terms according to eq A2 leads to the approximate relationship for the strong effector bound at equilibrium:

$$Y = L/[L + K'/K_0] \quad \text{(A4)}$$

The degree of desensitization I has been defined by Katz & Thesleff as an analogue to the allosteric state function:

$$I = [R' + R'L]/R_0 = R'Q'^{-1}/R_0 \quad \text{(A5)}$$

Following the same strategy as above, one derives:

$$I = (L + K')/(L + K'/K_0) \quad \text{(A6)}$$

which, in the case of $L \gg K' \simeq 70$ nM reduces to eq A4. Therefore, the fraction of ligand bound at equilibrium and the degree of desensitization follow approximately the same hyperbola, characterized by an apparent equilibrium constant K'/K_0, as long as the condition for a "strong effector" (eq A2) is fulfilled.

Coupling of Toxin Binding to the Two-State Model. Since the stoichiometry of toxin sites to Carb sites is 2:1 and R binds one Carb molecule, R can bind two toxin molecules, and the signal is given by

$$z = 2(RT + R'T + RT_2 + R'T_2) \quad \text{(A7)}$$

since the monotoxin complexes RT and R'T have a statistical weight of 2 (the two toxin sites on R and/or R' are identical and independent) and since the ditoxin complexes also count twice. We will show that under our experimental conditions (A) $R_0 \ll T_0, L_0$ and (B) $T_0 \ll R_0 \ll L_0$, the simplified writing of the competitive coupling of toxin binding to the Carb reaction (eq 3), where only one toxin molecule binding to R is considered, is justified.

(A) Kinetics with Toxin in Excess over Receptor. In the absence of ligand and with $T_0 \gg R_0$, the formation of z follows the rate equation:[2]

$$\dot{z} = kT_0\,(2R_0 - z)$$

since the toxin sites on R and R' are all identical and independent. If the receptor has been preequilibrated with ligand, Carb acts like a competitive inhibitor of toxin binding within the concentration range examined (see Figure 2). The kinetics of toxin binding are then described by the empirical formula (see text, eq 4).

$$\dot{z} = kT_0\,[1 + L/K_{app}]^{-1}(2R_0 - z) \quad \text{(A8)}$$

with $K_{app} = K'/K_0$ when starting with the low affinity form. The observed rate constant is again linear in T_0. Since for a strong effector the amount of ligand bound parallels the degree of desensitization I (see eq A4 and A6) eq A8 can be used for the determination of I.

In the case of a kinetic experiment (see Figure 1), AcChR and Carb are mixed at time $t = 0$ and toxin in excess is added at τ seconds after incubation. The initial slope of toxin binding $\dot{z}_{i\tau}$ will then be proportional to the amount of receptor not yet in the high affinity form:

$$\dot{z}_{i\tau} = \alpha T_0 R_0 (1 - I(\tau)) \quad \text{(A9)}$$

where α is a constant factor which depends on the particular kinetic mechanism chosen to describe the three component system. In the cases that (i) no ternary complexes between R, T, and L are formed or that (ii) only RL (but not R'L) can bind toxin with an arbitrary apparent rate $k'T_0$, one calculates:

$$\text{(i) } \alpha = Qk \text{ or (ii) } \alpha = Q[k + k'L/K] \quad \text{(A9a)}$$

(B) *Kinetics with Receptor in Excess over Toxin.* Under the conditions $T_0 \ll R_0 \ll L_0$ the rate of toxin binding can again be assumed to be proportional to the fraction of AcChR not yet in the high affinity form:

$$\dot{z} = \alpha T R_0\,(1 - I) = \alpha R_0\,(T_0 - z)\,(1 - I) \quad \text{(A10)}$$

where all toxin containing terms in the mass balance of receptor sites were neglected (since $T_0 \ll R_0$) and α is as explained in eq A9a. Integration of eq A10 with the initial condition $z(0) = 0$ leads to:

$$\ln\,[(T_0 - z)/T_0] = -\alpha R_0 t + \alpha R_0 \int_0^t I(t')dt' \quad \text{(A11)}$$

For I one derives the differential equation:

$$\dot{I} = R_0^{-1}\frac{d}{dt}(R' + R'L)$$

$$= R_0^{-1}\,[k_0 R - k_{-0}R' - k(T_0 - z)R' + k_1 RL - k_{-1}R'L]$$

Using $R' \simeq R_0 I Q'$, $R \simeq R_0 Q(1 - I)$ leads after rearrangement of terms to:

$$\dot{I} = -k_i I + Q[k_0 + k_1 L/K] \quad \text{(A12)}$$

where

$$k_i = Q[(k_0 + k)_1 L/K] + Q'[(k_{-0} + k_{-1})L/K'] + Q'k(T_0 - z) \quad \text{(A12a)}$$

Under our experimental conditions the toxin containing term is much smaller than the experimental values of k_i ($kT_0 \simeq 2 \times 10^{-4}\ M^{-1}\ s^{-1} \times 1 \times 10^{-7}\ M \ll 1.5 \times 10^{-2}\ s^{-1} < k_i$ at $[Carb]_0 > 5\ \mu M$, see Figure 4B) and it can be neglected in eq A12a, leading to the expression for the unperturbed system (Katz & Thesleff, 1957; Janin, 1973)

$$k_i = Q[(k_0 + k_1)L/K] + Q'(k_{-0} + k_{-1})L/K') \quad \text{(A13)}$$

Integration of eq A12 with $I(0) = I_0$ gives:

$$I(t) = (I_0 - I_\infty)\exp(-k_i t) + I_\infty \quad \text{(A14)}$$

with

$$I_\infty = Q[(k_0 + k_1)L/K]/k_i = \left[1 + \frac{1 + L/K}{K_0\,[1 + L/K']}\right]^{-1} \quad \text{(A15)}$$

which, in the case of a strong effector eq A2 reduces to eq A6. I_0 is the degree of desensitization at the moment when toxin is added and depends upon the experimental conditions. Inserting eq A14 in eq A11 and carrying out the integration yields:

$$\ln[(T_0 - z)/T_0] = -\alpha k_i^{-1} R_0\,(I_\infty - I_0) \times [1 - \exp(-k_i t)] - \alpha R_0[1 - I_\infty]t \quad \text{(A16)}$$

This equation shows that a semilog plot of $(T_0 - z)T_0$ vs. time consists of a rapid exponential decrease corresponding to the transition to high affinity form (k_i), followed by a slow linear decrease, corresponding to toxin binding to the high affinity receptor (see Figure 4A, time course b). Preincubation of receptor with ligand until the transition is complete gives $I(0) = I(\infty)$ and the transient term in eq A16 drops out (time course c in Figure 4A). Subtraction on a log scale of the linear term in A16 allows one to follow the kinetics of the unperturbed system and the semilog plot of $\ln[(T_0 - z)/T_0] + \alpha R_0[1 - I_\infty]t$ vs. t yields k_i as given in eq A13.

[2] Dot denotes derivative with respect to time.

References

Adams, P. R. (1975) *Pflugers Arch. 360,* 145-153.

Barrantes, F. J. (1976) *Biochem. Biophys. Res. Commun. 72,* 479.

Bevington, P. R. (1969) *Data Reduction and Error Analysis for the Physical Sciences,* McGraw Hill, New York, N.Y. (especially Section 9.3).

Bonner, R., Barrantes, F. J., & Jovin, T. M. (1976) *Nature (London) 263,* 429.

Changeux, J.-P., Benedetti, L., Bourgeois, J.-P., Brisson, A., Cartaud, J., Devaux, P., Grünhagen, H., Moreau, M., Popot, J., Sobel, A., & Weber, M. (1976) *Cold Spring Harbor Symp. Quant. Biol. 40,* 211.
Clark, D. G., Macmurchie, D. D., Elliot, E., Wolcott, R. G., Landel, A. M., & Raftery, M. A. (1972) *Biochemistry 11,* 1595.
Cohen, J., Weber, M., Huchet, M., & Changeux, J. P. (1972) *FEBS Lett. 26,* 43.
Colquhoun, D., & Rang, H. P. (1976) *Mol. Pharmacol. 12,* 519–535.
Duguid, J. R., & Raftery, M. A. (1973) *Biochemistry 12,* 3693.
Grünhagen, H. H., & Changeux, J. P. (1976) *J. Mol. Biol. 106,* 517.
Janin, J. (1973) *Prog. Biophys. Mol. Biol. 27,* 77–120.
Katz, B., & Thesleff, S. (1957) *J. Physiol. 138,* 63.
Lee, T., Witzemann, V., Schimerlik, M., & Raftery, M. A. (1977) *Arch. Biochem. Biophys. 183,* 57–63.
Lester, H. A. (1972) *Mol. Pharmacol. 8,* 632–644.
Mooser, G., Schulman, H., & Sigman, D. (1972) *Biochemistry 11,* 1595.
Popot, J. L., Sugiyama, H., & Changeux, J. P. (1976) *J. Mol. Biol. 106,* 469–483.
Quast, U., Schimerlik, M., & Raftery, M. A. (1978) *Biochem. Biophys. Res. Commun.* (in press).
Raftery, M. A., Vandlen, R. L., Reed, K. L., & Lee, T. (1975) *Cold Spring Harbor Symp. Quant. Biol. 40,* 193.
Rang, H. P., & Ritter, J. M. (1969) *Mol. Pharmacol. 5,* 394.
Rang, H. P., & Ritter, J. M. (1970a) *Mol. Pharmacol. 6,* 357.
Rang, H. P., & Ritter, J. M. (1970b) *Mol. Pharmacol. 6,* 383.
Reed, K., Vandlen, R., Bode, J., Duguid, J., & Raftery, M. A. (1975) *Arch. Biochem. Biophys. 167,* 138.
Schimerlik, M. I., & Raftery, M. A. (1976) *Biochem. Biophys. Res. Commun. 73,* 607.
Schmidt, J., & Raftery, M. A. (1973) *Anal. Biochem. 52,* 349.
Sheridan, R., & Lester, H. A. (1975) *Proc. Natl. Acad. Sci. U.S.A. 9,* 3496.
Weber, M., & Changeux, J. P. (1974a) *Mol. Pharmacol. 10,* 15–34.
Weber, M., & Changeux, J.-P. (1974b) *Mol. Pharmacol. 10,* 35.
Weber, M., David-Pfeuty, T., & Changeux, J. P. (1975) *Proc. Natl. Acad. Sci. U.S.A. 72,* 3443.
Weiland, G., Georgia, B., Wee, V. T., Chignell, C. F., & Taylor, P. (1976) *Mol. Pharmacol. 12,* 1091.
Weiland, G., Georgia, B., Lappi, S., Chignell, C. F., & Taylor, P. (1977) *J. Biol. Chem. 252,* 7648–7656.
Witzemann, V., & Raftery, M. A. (1977) *Biochemistry 16,* 5862.

Photogenerated Reagents for Membrane Labeling. 1. Phenylnitrene Formed within the Lipid Bilayer†

Hagan Bayley and Jeremy R. Knowles*

ABSTRACT: Phenylnitrene generated photochemically from phenyl azide that is bound to artificial phospholipid vesicles labels the fatty acid chains of the lipids in low yield. The labeling yield varies from approximately 3.3% with soybean lecithin (which is highly unsaturated) to approximately 0.25% with dimyristoyllecithin (which is completely saturated). Labeling is largely eliminated by reduced glutathione in the aqueous phase. Nitrenes are evidently unsatisfactory reagents for the labeling either of lipids or by analogy of the hydrophobic portions of membrane proteins. This is mainly because the long lifetimes and electrophilic character of nitrenes will lead to the preferential labeling of extrinsic membrane components. Phenyl azide itself is further compromised as a lipophilic reagent by its rather low partition coefficient into lipid bilayers, as measured by equilibrium dialysis.

During the past 10 years or so, a vague but nevertheless useful model for the structure of biological membranes has become accepted, in which proteins and glycoproteins are considered to be associated in various ways with a more or less fluid bilayer of lipid. The proteins and the lipids are vectorially arranged with respect to the two faces of the bilayer (the inside and the outside), and, of late, considerable effort has been devoted to the definition of this vectorial organization. Surface labeling of exposed membrane components using a variety of chemical reagents (Bretscher, 1971) continues to provide the most important information in this area (Hubbard & Cohn, 1976; Rothman & Lenard, 1977). Recently, photochemical surface labeling has been used in an attempt to overcome the reactivity limitations of ordinary chemical reagents (Staros & Richards, 1974).

The identification and characterization of membrane components situated *within* the bilayer have, however, been much less thorough. Such components may be whole molecules buried in the bilayer [e.g., small proteolipids (MacLennan et al., 1972)] or they may be parts of molecules [e.g., the hydrophobic tail of cytochrome b_5 (Spatz & Strittmatter, 1971), the hydrophobic peptide of glycophorin that is believed to cross the membrane (Marchesi et al., 1976), or multiply spanning segments as proposed for band 3 protein from human red blood cell membranes (Jenkins & Tanner, 1975)]. The location of such lipophilic components has been indirectly inferred from

† From the Department of Chemistry, Harvard University, Cambridge, Massachusetts 02138. *Received December 5, 1977.* This work was supported by the National Institutes of Health.

0006-2960/78/0417-2414$01.00/0